



## RAPID COMMUNICATION

# Transient HSP90 inhibition enhances the sensitivity of mantle cell lymphoma to poly (ADP-ribose) polymerase (PARP) inhibitors



Mantle cell lymphoma (MCL) is an aggressive subtype of non-Hodgkin lymphoma (NHL) characterized by the over-expression of cyclin D1 and deregulated cell cycle.<sup>1</sup> Ganetespib (STA-9090), a second-generation HSP90 inhibitor, dramatically disrupted oncogenic cellular processes resulting in the inhibition of client protein-derived tumors in preclinical studies.<sup>2</sup> The synthetic lethal strategy using poly (ADP-ribose) polymerase (PARP) inhibitors (PARPis) has been reported as a powerful therapeutic intervention in MCL and their effectiveness can be increased by a deficiency in DNA damage repair (DDR), especially homologous recombination deficiency.<sup>3</sup> Since we found earlier that transient ganetespib treatment can induce defects in DDR, we hypothesized that ganetespib treatment can possibly enhance the sensitivity of MCL cells to PARPis and HSP90 and PARP is can be demonstrated as promising combination therapies for MCL.

To assess the growth inhibitory activities of HSP90 and PARP inhibitors, MCL cells were treated with different concentrations of ganetespib or olaparib for 72 h. Ganetespib yielded IC<sub>50</sub> values of 12.84 ± 1.57 nM and 20.57 ± 3.34 nM for Jeko-1 and REC-1 cells, respectively (Fig. S1A, B). Olaparib yielded IC<sub>50</sub> values of 24.56 ± 3.65 μM and 50.68 ± 10.90 μM, respectively (Fig. S1C, D). Therefore, both ganetespib and olaparib effectively suppressed the growth of MCL cells.

Since HSP90 has hundreds of client proteins, we found that transient exposure to ganetespib for 12 h was sufficient to inhibit MCL cell growth, induce defects in DNA damage repair in MCL, and avoid complicated responses and toxicities *in vivo*. In addition, the sensitivity of cancer cells to PARPis can be increased by DNA repair deficiency; therefore, we tested whether transient pretreatment with ganetespib would increase the sensitivity of MCL cells to

PARP inhibition. Thus, Jeko-1 and REC-1 cells were first treated with ganetespib (or vehicle) at 15 nM and 20 nM according to their corresponding IC<sub>50</sub> values, respectively, for 12 h, and then ganetespib was removed and the cells were treated with olaparib for another 60 h (Fig. 1A). The IC<sub>50</sub> values of olaparib in the ganetespib-olaparib groups versus vehicle-olaparib groups were increased by 3.27-fold and 7.35-fold in Jeko-1 and REC-1 cells, respectively (Fig. 1B–D). Approval for the study was obtained from the Ethics Committee at Jiangsu University. The informed consent form was signed by the patients. Meanwhile, similar results were obtained when the primary cells from two MCL patients were treated with olaparib in combination with ganetespib (Fig. S2). These results supported that pretreatment of ganetespib sensitized MCL cells to the PARPi olaparib.

To explore the mechanism by which ganetespib pretreatment sensitized MCL cells to olaparib, Jeko-1 cells were pretreated with ganetespib at 15 nM for 12 h and then treated with olaparib at 25 μM for another 36 h (Fig. S3A). Ganetespib pretreatment significantly increased the percentage of apoptotic cells of the ganetespib-olaparib group compared with those of the other groups (Fig. 1E; Fig. S3B). Similar results were obtained when REC-1 cells were treated in this way (Fig. 1F; Fig. S3C). Moreover, the proportion of Jeko-1 cells in G2/M phases was significantly increased, and that in G0/G1 phases was significantly decreased when the distribution of cell cycle of the ganetespib-olaparib group was compared with that of the vehicle-olaparib group (Fig. 1G; Fig. S3D). Similar results were obtained when REC-1 cells were also treated (Fig. 1H; Fig. S3E). Western blot results showed the up-regulation of cleaved-caspase 3 and cleaved-PARP in MCL cells with ganetespib pretreatment, consistent with flow cytometry results (Fig. 1I). The protein levels of cyclin D1, CDK4, and cyclin A of the ganetespib-olaparib group were dramatically decreased when

Peer review under responsibility of Chongqing Medical University.

<https://doi.org/10.1016/j.gendis.2023.01.006>

2352-3042/© 2023 The Authors. Publishing services by Elsevier B.V. on behalf of KeAi Communications Co., Ltd. This is an open access article under the CC BY-NC-ND license (<http://creativecommons.org/licenses/by-nc-nd/4.0/>).

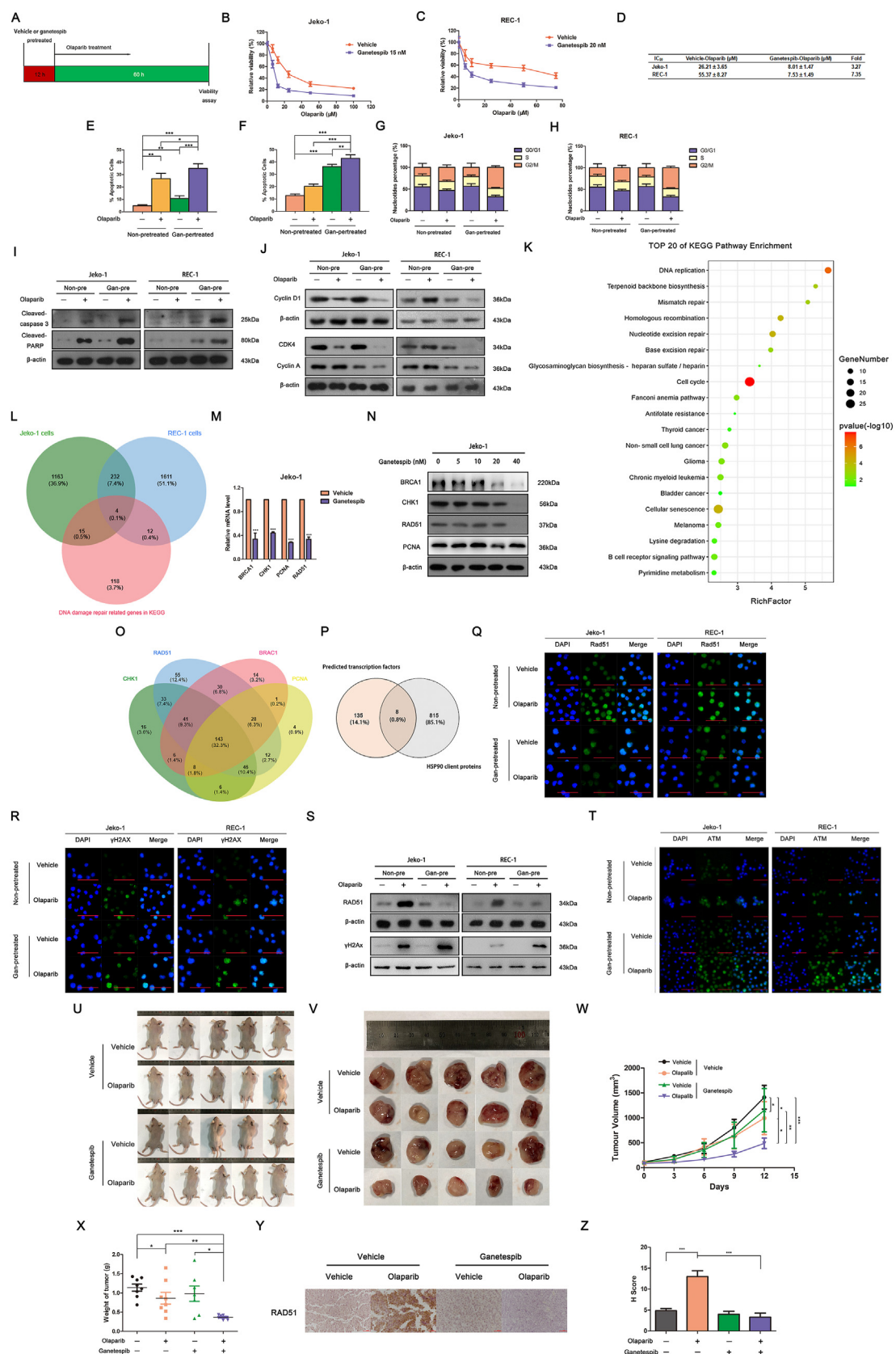


**Figure 1** Transient HSP90 inhibition enhances the sensitivity of mantle cell lymphoma to poly (ADP-ribose) polymerase (PARP) inhibitors. **(A)** The scheme of experiment settings for **(B, C)**. Cells were pretreated with either ganetespib at indicated concentration or vehicle for 12 h and then washed and cultured in media with olaparib for 60 h before cell viability was assessed by MTT assays. The relative viabilities of Jeko-1 and REC-1 cells treated with olaparib and pretreated with or without ganetespib were

compared with those of vehicle-olaparib group, consistent with the cell cycle results (Fig. 1J).

Next, to gain further insight into the molecular mechanisms of ganetespib pretreatment, transcriptome analysis on MCL cells was performed. The results of the KEGG pathway analysis showed that the differentially expressed genes after ganetespib pretreatment were enriched in DNA replication, mismatch repair, homologous recombination, and other pathways (Fig. 1K; Fig. S4A). Significant down-regulation was seen in 1414 genes in Jeko-1 cells and 1859 genes in REC-1 cells. A curated list of 149 genes involved in the key DDR-related pathways, such as nucleotide excision repair, base excision repair, mismatch repair, and homologous recombination,<sup>4</sup> were extracted from the KEGG database. Interestingly, among these DDR-related genes, *BRCA1*, *CHK1*, *PCNA*, and *RAD51* were consistently down-regulated in both MCL cell lines (Fig. 1L). Their mRNA expression all significantly decreased with ganetespib pretreatment in both cell lines (Fig. 1M; Fig. S4B), and their protein levels also significantly decreased (Fig. 1N; Fig. S4C). This indicated that ganetespib pretreatment down-regulated key genes involved in DNA double-strand break (DSB) repair. To gain insight into the mechanisms by which ganetespib treatment down-regulated transcription of the above genes, the Genecards database was used to build a library of the TF candidates of these genes; 143 common TFs were

identified with potential binding sites in promoter sequences of these genes (Fig. 1O). Among these TF candidates, the existing literature showed that eight TFs, namely, E2F1, HCFC1, IRF2, NFIC, MAX, PRDM1, REST, and ZBTB20 were also client proteins of HSP90 (Fig. 1P).

Given that ganetespib treatment down-regulated *BRCA1*, *CHK1*, *PCNA*, and *RAD51*, key players in DNA DSB repair, we further investigated the mechanism by which ganetespib treatment affected the sensitivity of MCL cells to olaparib via DNA repair pathways. The expression of *RAD51*,  $\gamma$ -H2AX foci, and ataxia-telangiectasia mutated (ATM), which were biomarkers of HR repair, unrepaired DSBs, and the earliest kinase activated when cells respond to DSB, respectively, was evaluated. The results of immunofluorescence and Western blot indicated a significant decrease in *RAD51* expression and a significant accumulation of  $\gamma$ H2AX foci when cells were sequentially treated with ganetespib and olaparib versus vehicle and olaparib (Fig. 1Q–S; Fig. S5A, B). Moreover, ATM levels significantly increased when cells were treated with combined ganetespib and olaparib compared with those of the cells treated only with olaparib (Fig. 1T; Fig. S5C). Together, these data suggest that transient ganetespib treatment can inhibit HR repair activity and increase the accumulation of DNA damage.

The effects of combined ganetespib and olaparib were then tested *in vivo*. All procedures involving mice were

shown in (B) and (C), respectively. For pretreatment of ganetespib, ganetespib (DMSO was used in the vehicle group) was applied on cells (15 nM for Jeko-1 and 20 nM for REC-1) for 12 h and then washed. After that, cells were cultured in media with olaparib at different concentrations for another 60 h. (D) The IC<sub>50</sub> values were calculated by using data from (B) and (C). (E–J) Cells were pretreated with either ganetespib at indicated concentration or vehicle for 12 h and then washed and cultured in media with olaparib for 36 h before the cell cycle, apoptosis assay, and Western blot analysis. (E, F) Cells were stained with annexin V–FITC/propidium iodide and analyzed for apoptosis distribution. Analyzed results of the presence of apoptotic cells of flow cytometry plots of Jeko-1 and REC-1 cells after different treatments were presented in (E) and (F), respectively. (G, H) Cells were stained with propidium iodide. Statistics of cell cycle distribution of Jeko-1 and REC-1 cells after different treatments were presented in (G) and (H), respectively. (I) The expression levels of cleaved-PARP and cleaved-caspase 3 were measured by Western blot. (J) The expression levels of cell cycle-associated proteins, including cyclin D1, CDK4, and cyclin A were detected by Western blot.  $\beta$ -Actin was used as an inner control. (K) The KEGG pathway enrichment analysis of total RNAs from Jeko-1 cells with transient ganetespib treatment for 12 h. Dot plots show the top 20 significantly enriched KEGG pathways. Point size corresponds to the gene numbers involved in the corresponding KEGG pathway, and points are plotted horizontally according to the rich factors. Their colors are shown by *P*-values. (L) The Venn diagram created based on the DNA damage-related genes whose expression levels were down-regulated in two MCL cell lines as indicated. (M) The mRNA expression of *BRCA1*, *CHK1*, *PCNA*, and *RAD51* in Jeko-1 cells with transient ganetespib treatment. (N) The protein levels of *BRCA1*, *CHK1*, *RAD51*, and *PCNA* in Jeko-1 with transient ganetespib treatment for 12 h.  $\beta$ -Actin was used as an inner control. (O) The Venn diagram created based on the transcription factors (TFs) identified with the potential binding sites in promoter sequences of the *RAD51*, *BRCA1*, *CHK1*, and *PCNA* via the Genecards database. (P) The Venn diagram created based on TF candidates which were also the client proteins of HSP90. (Q–T) Cells were pretreated with either ganetespib at indicated concentration or vehicle for 12 h and then washed and cultured in media with olaparib for 36 h. The *RAD51* and  $\gamma$ -H2AX levels were analyzed by immunofluorescence, and cells exhibiting *RAD51* and  $\gamma$ -H2AX foci with positive staining were shown in (Q) and (R), respectively. The scale bar represents 20  $\mu$ m. (S) The protein levels of *RAD51* and  $\gamma$ -H2AX in Jeko-1 and REC-1 cells after treatments. (T) The protein level of ATM was analyzed by immunofluorescence, and the cells exhibiting ATM-positive staining were shown. The scale bar represents 20  $\mu$ m. (U–Z) Over a period of 12 days, mice bearing Jeko-1 xenografts ( $n = 6$ /group) were randomized into four treatment groups ( $n = 5$ ) and treated intravenously with 25 mg/kg ganetespib (or vehicle) once weekly or/and treated intraperitoneally with 50 mg/kg olaparib (or vehicle) daily, starting when the tumor volume reached about 100 mm<sup>3</sup>. The representative pictures of xenografts bearing mice and tumors after 12 days of treatment were shown in (U) and (V). (W) The tumor sizes were measured every day and shown as tumor volume (mean  $\pm$  SD) over time. (X) Tumor weights were measured after sacrifice. (Y) The representative pictures of immunohistochemistry detections of *RAD51* in tumors with different treatments. (Z) Statistics of immunohistochemistry detections of *RAD51* in (Y). The scale bar represents 50  $\mu$ m. The data shown are the mean  $\pm$  SD from three independent experiments. Statistically significant differences with  $P < 0.05$  were considered significant (\* $P < 0.05$ , \*\* $P < 0.01$ , \*\*\* $P < 0.001$ ).

approved by the Institutional Animal Care and Use Committee of Jiangsu University. The results demonstrated that weekly administration of ganetespib (25 mg/kg) followed by daily administration of olaparib (50 mg/kg) dramatically inhibited the growth of xenograft tumors (Fig. 1U–X; Fig. S6A). Immunohistochemistry results indicated that combination treatment greatly reduced levels of RAD51 in tumors compared with the olaparib alone group (Fig. 1Y, Z). The heart, liver, kidney, lung, and spleen were weighed, and no significant changes were found in these major organs of mice (Fig. S6B–F). H&E staining of the liver and kidney also showed no significant change in the toxicity of combination therapy (Fig. S6G). These data demonstrated that ganetespib enhances the effects of olaparib on inhibiting tumor growth by decreasing DNA HR repair in the xenograft tumor model.

To date, there is no standard frontline therapy for MCL. The synthetic lethal approach using PARPis has been reported as a powerful therapeutic intervention for treating MCL. To expand the benefits of PARPis in MCL, there has been considerable interest in identifying targeted agents that can be combined in patients without DNA repair deficiency. Ganetespib can effectively destabilize the key DNA repair proteins, making it a promising candidate agent for combination use with olaparib. This study demonstrates that ganetespib and olaparib may serve as a promising drug combination for MCL treatment.

### Author contributions

CS wrote the manuscript and performed analysis. DR and YG carried out experiments and performed analysis. ZT and HL supervised, designed the study, and wrote the manuscript. YD performed analysis and assisted in writing the manuscript. All authors read and approved the final manuscript.

### Conflict of interests

The authors declare that they have no competing interests.

### Funding

This work was supported by the National Natural Science Foundation of China (No. 81672582 to HL, 31771521 to ZT, and 82200083 to CS), Top Talent of Innovative Research Team of Jiangsu Province, China (to HL and ZT), the Natural

Science Foundation of Jiangsu Province, China (No. BK20200891 to CS), and the Senior Talent Start-up Funds of Jiangsu University (China) (No. 14JDG050 and 14JDG011 to HL and ZT).

### Appendix A. Supplementary data

Supplementary data to this article can be found online at <https://doi.org/10.1016/j.gendis.2023.01.006>.

### References

1. Rosenwald A, Wright G, Wiestner A, et al. The proliferation gene expression signature is a quantitative integrator of oncogenic events that predicts survival in mantle cell lymphoma. *Cancer Cell*. 2003;3(2):185–197.
2. Proia DA, Bates RC. Ganetespib and HSP90: translating preclinical hypotheses into clinical promise. *Cancer Res*. 2014;74(5):1294–1300.
3. Williamson CT, Muzik H, Turhan AG, et al. ATM deficiency sensitizes mantle cell lymphoma cells to poly(ADP-ribose) polymerase-1 inhibitors. *Mol Cancer Ther*. 2010;9(2):347–357.
4. Tubbs A, Nussenzweig A. Endogenous DNA damage as a source of genomic instability in cancer. *Cell*. 2017;168(4):644–656.

Chaowen Shi <sup>a,1</sup>, Dewan Ren <sup>b,1</sup>, Yufeng Gao <sup>a</sup>, Ya-Mei Dang <sup>c</sup>, Zhigang Tu <sup>a,\*\*</sup>, Hanqing Liu <sup>b,\*</sup>

<sup>a</sup> School of Life Sciences, Jiangsu University, Zhenjiang, Jiangsu 212013, China

<sup>b</sup> School of Pharmacy, Jiangsu University, Zhenjiang, Jiangsu 212013, China

<sup>c</sup> Department of Pathology, Gansu Provincial Hospital, Lanzhou, Gansu 730000, China

\*Corresponding author. School of Pharmacy, Jiangsu University, 301 Xuefu Road, Jingkou District, Zhenjiang, Jiangsu 212013, China.

\*\*Corresponding author. School of Life Sciences, Jiangsu University, 301 Xuefu Road, Jingkou District, Zhenjiang, Jiangsu 212013, China.

E-mail addresses: [zhigangtu@ujs.edu.cn](mailto:zhigangtu@ujs.edu.cn) (Z. Tu), [hanqing@ujs.edu.cn](mailto:hanqing@ujs.edu.cn) (H. Liu)

2 June 2022

Available online 21 April 2023

<sup>1</sup> These authors contributed equally to this study.